AJNR

Synthetic MRI in Neurofibromatosis Type 1

G. Coban, S. Parlak, E. Gumeler, H. Altunbuker, B. Konuskan, J. Karakaya, B. Anlar and K.K. Oguz

AJNR Am J Neuroradiol published online 15 July 2021
http://www.ajnr.org/content/early/2021/07/15/ajnr.A7214

Published July 15, 2021 as 10.3174/ajnr.A7214

Synthetic MRI in Neurofibromatosis Type 1

G. Coban, S. Parlak, E. Gumeler, H. Altunbuker, B. Konuşkan, J. Karakaya, B. Anlar, and K.K. Oguz

ABSTRACT

BACKGROUND AND PURPOSE: Synthetic MRI enables the generation of various contrast-weighted images and quantitative data in a reasonable scanning time. We aimed to use synthetic MRI to assess the detection and underlying tissue characteristics of focal areas of signal intensity and normal-appearing brain parenchyma and morphometric alterations in the brains of patients with neurofibromatosis type 1.

MATERIALS AND METHODS: Conventional MR imaging and synthetic MRI were prospectively obtained from 19 patients with neurofibromatosis type 1 and 18 healthy controls. Two neuroradiologists independently evaluated focal areas of signal intensity on both conventional MR imaging and synthetic MRI. Additionally, automatically segmented volume calculations of the brain in both groups and quantitative analysis of myelin, including the focal areas of signal intensity and normal-appearing brain parenchyma, of patients with neurofibromatosis type 1 were performed using synthetic MRI.

RESULTS: The comparison of conventional MR imaging and synthetic MRI showed good correlation in the supratentorial region of the brain ($\kappa = 0.82–1$). Automatically segmented brain parenchymal volume, intracranial volume, and GM volumes were significantly increased in the patients with neurofibromatosis type 1 ($P < .05$). The myelin-correlated compound, myelin fraction volume, WM fraction volume, transverse relaxation rate, and longitudinal relaxation rate values were significantly decreased in focal areas of signal intensity on myelin and WM maps ($P < .001$); however, GM, GM fraction volume, and proton density values were significantly increased on the GM map ($P < .001$).

CONCLUSIONS: Synthetic MRI is a potential tool for the assessment of morphometric and tissue alterations as well as the detection of focal areas of signal intensity in patients with neurofibromatosis type 1 in a reasonable scan time.

ABBREVIATIONS: BPF = brain parenchymal fraction; BPV = brain parenchymal volume; cMRI = conventional MRI; FASI = focal areas of signal intensity; GMFvol = mean amount of GM within a single voxel; HC = healthy control; ICV = intracranial volume; MY = myelin; MyCvol = myelin correlated fraction volume; MyF = myelin fraction; MyV = myelin correlated volume; NABP = normal-appearing brain parenchyma; NF-1 = neurofibromatosis type 1; NoN, non-GM/WM/CSF; PD = proton density; QRAPMASTER = quantification of relaxation times and proton density by multiecho acquisition of a saturation-recovery using turbo spin-echo readout; R1 = longitudinal relaxation rate; R2 = transverse relaxation rate; SyMRI = synthetic MRI; WMFvol = the mean amount of WM within a single voxel

Neuroimaging plays an important role in the diagnosis and follow-up of neurofibromatosis type 1 (NF-1). The most common parenchymal abnormality of the brain in NF-1 is oval or round focal areas of abnormal signal intensity (FASI), mainly in the basal ganglia, cerebellum, and brain stem on T2WI. These lesions do not show enhancement with gadolinium or mass effects.[1] Additionally, studies in *Drosophila* species and mice with *NF1* gene mutations have shown progressive myelin (MY) defects and behavioral abnormalities in a *neurofibromin 1* dose-dependent fashion.[2-4] Although evidence is inconclusive, vacuolar changes in myelin, defined as fluid-containing spaces ranging from 5 to 100 mm, have been suggested to explain the FASI.[5,6]

The synthetic MRI (SyMRI) sequence, called quantification of relaxation times and proton density by multiecho acquisition of a saturation-recovery (QRAPMASTER) using turbo spin-echo readout,[7] enables automatic segmentation of brain tissue and measurement of myelin-based quantitative values with good accuracy and reproducibility in approximately 6 minutes with full head coverage.[8] This sequence has had encouraging results for brain metastasis,

Received January 9, 2021; accepted after revision April 19.

From the Departments of Radiology (G.C., S.P., E.G., K.K.O.), Biostatistics (J.K.), and Pediatric Neurology (B.A.), Hacettepe University School of Medicine, Ankara, Turkey; Istanbul İl Ambulans Servisi Başhekimliği, (H.A.), Istanbul, Turkey; and Department of Pediatric Neurology (B.K.), Mardin State Hospital, Mardin, Turkey.

Please address correspondence to Gokcen Coban, MD, Hacettepe Universitesi Tıp Fakültesi Hastanesi 06100 Sıhhiye, Department of Radiology, Ankara, Turkey; e-mail: drgokcencoban@gmail.com

Indicates article with online supplemental data.

http://dx.doi.org/10.3174/ajnr.A7214

multiple sclerosis, meningitis, idiopathic normal pressure hydrocephalus, and Sturge-Weber syndrome in several studies and has been approved by the FDA.[8-12]

In this study, we aimed to detect and evaluate FASI and examine morphometric changes in the brain in patients with NF-1 using SyMRI. We also sought myelin abnormalities in FASI and normal-appearing brain parenchyma (NABP) in patients with NF-1. Because FASI tends to resolve by early adulthood, we intentionally performed this study with pediatric patients.[13] Our hypothesis was that SyMRI could detect FASI and quantify morphologic and tissue changes in pediatric patients with NF-1.

MATERIALS AND METHODS

The institutional review board of Hacettepe University School of Medicine approved this prospective study (no = KA-180135). Patients' parents signed an informed consent form.

Ethics Approval

All procedures performed in the studies involving human participants were in accordance with the ethical standards of the institutional and/or the national research committee and with the 1964 Declaration of Helsinki and its later amendments or comparable ethical standards.

Participants and Image Acquisition

Between August 2019 and March 2020, pediatric patients fulfilling the NF-1 diagnostic criteria of the National Institutes of Health participated in this study at Hacettepe University School of Medicine. These patients were diagnosed and followed up by the Pediatric Neurology Department in our hospital, which has served as a reference center for patients with NF-1 in the past decade. Twenty-four patients with NF-1 fulfilling the diagnostic criteria were referred from the Pediatric Neurology Department and scanned in the Radiology Department. Twenty two healthy controls (HCs) without neurologic and systemic abnormalities volunteered to serve as the control group of the study. The exclusion criteria were the presence of optic glioma and brain tumors, hydrocephalus, increased head circumference, and chronic epilepsy in the NF-1 group and any incidental abnormality of the brain parenchyma in HCs. Individuals with reduced image quality on SyMRI or conventional MR imaging (cMRI) were eliminated from the study. One patient with NF-1 with a parenchymal tumor, 3 patients with NF-1 with optic gliomas, and 1 patient with NF-1 and 1 healthy control with reduced image quality were excluded from the study. Thus, of 24 patients with NF-1 and 22 HCs, 19 patients with NF-1 and 18 HCs were included in the study. None of the 37 participants received sedation or contrast media.

All scans were obtained on a 1.5T MR imaging scanner (Aera; Siemens) using a 20-channel phased array head coil. Conventional MR imaging protocol included axial FLAIR (TE/TR/TI, 78/7000/2220 ms; FOV, 230 × 185 mm; section thickness/gaps, 5/2 mm; acquisition time, 4 minutes 6 seconds); axial 3D T1-weighted MPRAGE (TE/TR, 3/1680 ms; FOV, 240 × 195 mm; section thickness/gaps, 1.5/0.75 mm; acquisition time, 5 minutes 8 seconds); and axial T2-weighted turbo spin-echo (TE/TR, 199/3240 ms; FOV, 230 × 185 mm; section thickness/gaps, 5/2 mm; acquisition time, 3 minutes 42 seconds).

The quantitative sequence QRAPMASTER[7] is a multi-spin-echo saturation-recovery sequence with multisaturation delays and multisections. The SyMRI technique was performed with the following parameters: axial plane; FOV, 230 × 183 mm; voxel size, 1.5 × 1.5 mm; TE, 14, 28, 42, 56, 70 ms; TR, 4.244 seconds; TI, 0.0974, 0.5846, 1.8511, 4.0919 seconds; saturation flip angle, 120°; and acquisition time, 6 minutes 5 seconds. The full brain was covered with 30 slices with 4-mm thickness and a 1-mm gap.

The SyMRI technique was performed after cMRI. The total scanning time was 12 minutes 56 seconds for cMRI and 6:05 min for SyMRI in our study protocol.

Image Analysis

SyMRI diagnostic software, Version 11.2 (SyntheticMR) was used to create synthetic images and quantify intracranial volume (ICV), brain parenchymal volume (BPV), brain parenchymal fraction (BPF = BPV/ICV), GM, WM, CSF, non-GM/WM/CSF, MY, and myelin fraction (MyF = MY/BPV).[14] Additionally, SyMRI enabled the creation of variable contrast-weighting images while quantifying the longitudinal relaxation rate (R1), transverse relaxation rate (R2), and proton density (PD). The MR imaging acquisition voxel is composed of 4 partial volume compartments: the myelin partial volume, free water partial volume, cellular partial volume, and excess parenchymal water partial volume. The sum of the 4 compartments is 100%, and each partial volume compartment content can range from 0% to 100%.[15] Each partial volume compartment has its own relaxation properties and can be described by its R1, R2, and PD values. By using this approach, SyMRI can estimate the myelin volume in a voxel. The total volume of WM, GM, CSF, non-GM/WM/CSF, and myelin can be calculated by multiplying the summed volume fractions for each tissue type based on predefined tissue characteristics.[15] Additionally, the non-GM/WM/CSF represents the tissue not classified as GM, WM, and CSF and contains flow voids in larger blood vessels.

Qualitative Evaluation

Two blinded neuroradiologists (G.C. and S.P.) independently evaluated the cMRI and SyMRI sets on a standard imaging workstation. The presence and location of FASI on T2WI of cMRI and SyMRI were noted with a 2-week gap. The largest FASI was chosen in consensus for the quantitative analysis. To search for any relationship between FASI and brain morphometry, we grouped the patients by the number of FASI into 4 groups: group 1 (from 1 to 5), group 2 (from 6 to 10), group 3 (from 11 to 15), and group 4 (>15).

Quantitative Evaluation

The raw image dataset was transferred to an imaging workstation (syngo.via; Siemens). SyMRI produced quantification and colored maps of WM, GM, CSF, and myelin correlated volume (MyV). To avoid misalignment, we copied ROIs drawn on an image set to the contralateral side with the mirror copy option available in the SyMRI diagnostic software, Version 11.2.

Table 1: cMRI versus SyMRI and interobserver agreement for FASI detection[a]

	cMRI vs SyMRI (Ob1)	cMRI vs SyMRI (Ob2)	İnterobserver Agreement on SyMRI	İnterobserver Agreement on cMRI
Thalami	0.9	0.86	0.82	0.94
WM (centrum semiovale)	1	1	1	1
BG	1	1	1	1
Pons	1	0.94	0.9	0.98
Mesencephalon	1	0.92	0.9	0.94
Cerebellum and MCP	0.85	0.84	0.80	0.90
Peridentate area	0.56	0.72	0.65	0.82

Note:—Ob indicates observer; BG, basal ganglia; MCP, middle cerebellar peduncle.
[a] Weighted κ analysis.

First, MY colored maps were overlaid on the T2WI of the SyMRI technique, and the ROIs ranging from 0.2 to 0.6 mL were drawn from the globus pallidum, caudate nucleus, internal capsule, putamen, thalamus in the right and left hemispheres and from the center of the pons and midbrain on the colored myelin maps in patients and HCs (Online Supplemental Data). For NABP, ROIs were placed on a nonlesioned region of each centrum semiovale.

In addition, for the quantitative comparison of the FASI and the side, MY colored maps were overlaid on the T2WI from the SyMRI technique, and the ROI (0.2 mL) was drawn on the FASI. The ROI on the FASI was copied to the contralateral NABP. Then, the same measurements were made on the colored WM and GM maps. Measurements were excluded if bilateral FASI were present in the relevant structures. The amounts of MyV, WM, GM, PD, R2, and R1 within the ROIs were noted. Then, these ROIs also yielded myelin correlate fraction volume (MyCvol), the mean amount of WM within a single voxel (WMFvol), and mean amount of GM within a single voxel (GMFvol), which represented the mean amount of MyV, WM, and GM within a single voxel, respectively.

Statistical Analysis

Quantitative variables were evaluated with the Kolmogorov-Smirnov test to reveal the presence of normal distribution. Descriptive statistics were expressed as mean (SD) if variables were normally distributed or median (minimum-maximum) if variables did not show normal distribution. An independent-samples *t* test was used for variables (BPV, ICV, WM, GM, MY, %MY/BPV, %GM/ICV, %MY/ICV, R2) with normal distribution, and the Mann-Whitney *U* test was used for non-normally distributed variables. Comparison of the FASI and NABP (MyCvol, MyV, GMFvol, GM, WMFvol, WM and PD, and R2 and R1 of the MY, GM, and WM) was made with the Wilcoxon test.

For comparisons of continuous variables (BPV, ICV, WM, GM, MY, %MY/BPV, %GM/ICV, %MY/ICV, R2), the adjusted *P* value was obtained using the Benjamini-Hochberg method.[16]

Among categoric variables, groups were compared using the χ^2 test. The relationship of continuous and ordinal variables with each other was examined with the Spearman ρ correlation coefficient.

Interobserver agreement for MR imaging features was assessed with weighted κ analysis. In terms of agreement, the κ value was interpreted as poor (< 0.20), fair (0.21–0.40), moderate (0.41–0.60), good (0.61–0.80), or very good (0.81–1.00). Confidence intervals of the κ values were used to find possible nonoverlapping intervals.

All analyses were performed using SPSS Statistics 23.0 software (IBM) and the R 3.6.3 program (http://www.r-project.org/). A P value < .05 was considered statistically significant.

RESULTS

There were no statistically significant differences in terms of sex ($P = .159$) or age ($P = .221$) between the patients with NF-1 (female/male: 9:10; mean age, 10.5 [SD, 3.7] years; range, 5–17 years) and HCs (female/male: 12:6; mean age, 11 [SD, 3] years; range, 5–16 years). The demographic characteristics of the patients with NF-1 are given in the Online Supplemental Data.

Qualitative Evaluation

Interobserver agreement for the detection of FASI on SyMRI is provided in Table 1. Raters' detection of FASI on SyMRI was highly correlated in the supratentorial part of the brain (ie, the centrum semiovale, thalamus, and basal ganglia) ($\kappa = 0.82$-1) (Fig 1), while it was lower in the infratentorial part (especially in the cerebellum and middle cerebral peduncle and peri-dentate area, Online Supplemental Data) ($\kappa = 0.65$–0.85). The interobserver correlation was lowest in the peri-dentate area ($\kappa = 0.65$) (Fig 1*E*, -*F*). Additionally, the raters noticed that small FASI were not detectable on SyMRI, though they were readily seen on cMRI. Although the raters did not measure the size of the FASI individually, they noticed that those lesions undetected on non-GM/WM/CSF colored maps were <5 mm in diameter. In total, there were 33 FASI of <5 mm in 18 patients with NF-1.

The FASI in patients with NF-1 were in the basal ganglia ($n = 27$), thalamus ($n = 28$), cerebellum and middle cerebellar peduncle ($n = 17$), peri-dentate area ($n = 23$), pons ($n = 19$), mesencephalon ($n = 17$), and cerebral white matter ($n = 2$) on cMRI. By categorization of the number of FASI, there were 6 patients in group 1, nine patients in group 2, three patients in group 3, and 1 patient in group 4. There was no significant correlation between the number of FASI and total brain MY, MyF, BPV, ICV, BPF, WM, GM, and non-WM/GM/CSF volumes.

Quantitative Evaluation

Total brain MY, MyF, BPV, ICV, BPF, WM, GM, and non-WM/GM/CSF volumes and MyV, MyCvol, PD, and R2 and R1 values of the centrum semiovale, globus pallidum, caudate nucleus,

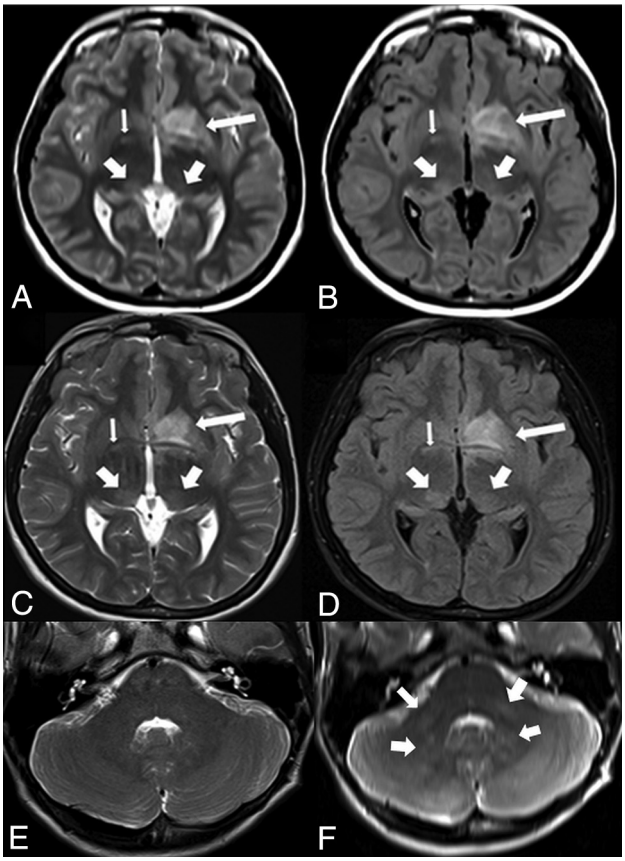

FIG 1. Synthetic T2-weighted (*A*) and FLAIR (*B*) images show FASI in the left lentiform nucleus, right globus pallidus, and bilateral thalami, accurately, as shown on the conventional T2-weighted (*C*) and FLAIR (*D*) images. T2-weighted image (*E*) in an HC shows no lesion in the peri-dentate area. However, a hyperintensity is seen in the corresponding area on synthetic T2-weighted image (*F*, *arrows*), an artifact probably due to CSF flow.

Table 2: Comparison of SyMRI parameters of patients with NF-1 and healthy controls

Variables	Healthy Controls		NF-1		*P* Value[a]
	Mean	SD	Mean	SD	
BPV (mL)	1279	109.64	1390	131.23	.035[b]
ICV (mL)	1401	120.16	1510	138.67	.035[b]
WM (mL)	396.20	66.78	419.88	48.83	.286
GM (mL)	862.93	82.29	949.16	89.15	.028[b]
MY (mL)	107.96	14.37	129.27	17.25	.067
%MY/BPV	8.53	0.85	8.51	0.80	.933
%GM/ICV	61.72	4.65	62.26	2.02	.763
%MY/ICV	7.80	0.82	7.87	0.82	.832
R GP R2[c]	14.49	1.02	13.66	1.31	.062
R CN R2	12.15	0.38	11.82	0.52	.058
L CN R2	12.12	0.37	11.74	0.56	.042[b]
R thalamus R2	12.74	0.39	12.34	0.52	.035[b]
L thalamus R2	12.69	0.38	12.28	0.51	.035[b]
Pons MyV (mL)	21.96	3.01	18.54	3.73	.028[b]

Note:—GP indicates globus palladium; CN, caudate nucleus; R, right; L, left.
[a] Independent-samples *t* test; adjusted *P* value was obtained using the Benjamini-Hochberg method.
[b] Significance is <.05.
[c] R2 unit is s-1.

putamen, thalamus, and internal capsule from the right and left hemispheres and the centrum of the pons and midbrain of HCs and the NF-1 patient group are provided in the Online Supplemental Data.

Brain parenchymal volume, ICV, and GM volumes (Table 2) were significantly increased in patients with NF-1 ($P < .05$) compared with HCs (Table 2). However, measurements from the aforementioned predetermined regions detected no differences between HCs and patients.

Conversely, MyV, MyCvol, WM, WMFvol, and R2, and R1 values were significantly decreased in the FASI compared with the NABP (Table 3, $P < .001$) (Fig 2). GM, GMFvol, and PD values were significantly increased on GM maps in FASI (Table 3, $P < .001$). FASI were automatically labeled only on the colored GM map, similar to the cortex, and not labeled and calculated on WM and MY maps (Fig 2). There was no significant difference in terms of MyV, MyCvol, PD, and R2 and R1 values of NABP (centrum semiovale) between patients and HCs ($P > .05$).

DISCUSSION

This study presents the first quantitative and qualitative analyses with SyMRI in patients with NF-1. Similar to findings of authors of recent studies testing lesion detection in multiple sclerosis with SyMRI,[12,17] we found that FASI were more easily detected on conventional T2- and FLAIR-weighted imaging. This finding could be related to lower image contrast, higher noise level, and hence lower contrast/noise ratio of synthetic FLAIR images compared with conventional images.[12,17] Nevertheless, previous studies showed that the diagnostic ability of SyMRI was comparable with that of cMRI, and they have suggested its clinical use in various diseases.[8,12] We also found a good correlation between cMRI and SyMRI in the detection of FASI in patients with NF-1, supporting the use of SyMRI in routine practice. Posterior fossa structures, especially the peridentate area, had the lowest interobserver correlation. The major reason for this low correlation was the prominent artifacts due to phase-encoding and fluid-pulsation artifacts in the infratentorial compartment, also mentioned in the literature.[18,19] Kerleroux et al[19] showed that phase-encoding and fluid-pulsation artifacts were more common in synthetic T2WI than in T2WI on cMRI. However, they noted that the phase-encoding artifacts were easily recognizable and should not be confounded with pathologic conditions. However, fluid-pulsation artifacts might disturb the evaluation of lower brain areas, such as the brain stem or peduncles, in both patients and HCs. Given this limitation of SyMRI, we believe that cMRI is necessary for initial imaging to avoid misinterpretation. On SyMRI, non-GM/WM/CSF maps could not assign FASI that were <5 mm in diameter in our patients, though the raters were able to detect them easily.

The Pediatric Neurology Department of our hospital serves as a reference center for patients with NF-1. During the annual checkups of patients with NF-1, follow-up imaging is required; therefore, brain MR imaging examinations are performed in our neuroradiology department. Most patients cannot tolerate the long imaging time due to accompanying cognitive and neuropsychiatric disorders. With SyMRI, annual checkups can be performed in a shorter time after the baseline cMRI examination,

Table 3: ROI analysis of FASI and normal-appearing WM on MYC, GM, and WM maps, testing MyV, PD, R2, R1, GM, WM, and MyC/WM/GM fractional volumes[a]

	Normal-Appearing White Matter		FASI		
Variables	Median	Min-Max	Median	Min-Max	*P* Value[b]
MyCvol (mL)	0.03	0.01–0.05	0.000	0.00–0.002	.001
MyV (mL)	14.1	6.9–29.9	2.5	0–18.7	.001
MY PD	76.4	66–81.1	83.3	73.2–89	.001
MY R2	12.6	11.19–15.2	10.36	7.08–13.85	.001
MY R1	1.22	1.05–1.76	0.96	0.73–1.27	.001
WMFvol (mL)	0.13	0.05–0.17	0.02	0.00-0.13	.001
WM	64.3	26.7–100	2.7	0.00–73.5	.001
WM PD	76.4	66–80	83.3	51.1–87.8	.001
WM R2	12.6	11.19–15.22	10.36	1.99–76.1	.001
WM R1	1.21	1.05-1.76	0.96	0.73–12.31	.001
GMFvol (mL)	0.06	0.00–0.13	0.11	0.05-0.21	.001
GM	29.2	0.00–70.1	75.2	14.8–86.1	.001
GM PD	76.4	66–81.9	83.3	73.2–90.51	.001
GM R2	12.6	11.19–15.22	10.36	0.9–13.85	.001
GM R1	1.2	1.05–1.76	0.96	0.73–1.27	.001

Note:—Min indicates minimum; Max, maximum; MyC, myelin correlated fraction volume.
[a] Units are PD (PU), R1 and R2 (s-1), WM (mL), GM (mL).
[b] Wilcoxon test.

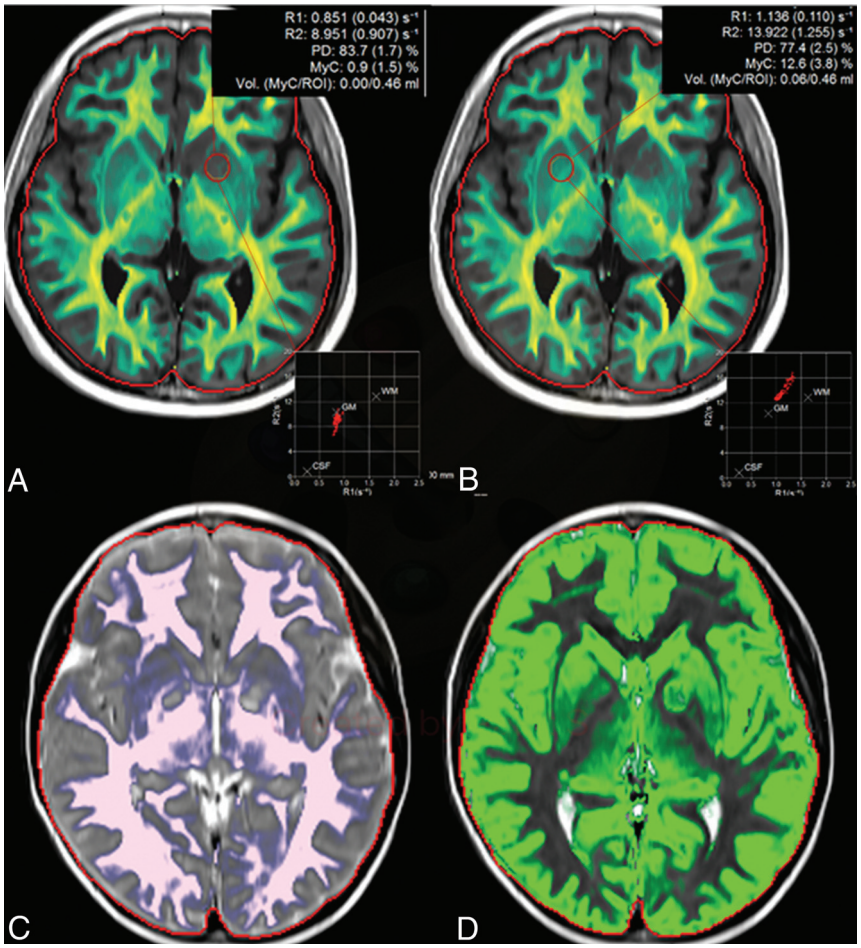

FIG 2. Myelin (*A* and *B*), WM (*C*), and GM (*D*) maps of a patient with NF-1. FASI in the left lentiform nucleus (*A*, *red ROI*) show prominently decreased R1, R2, PD, MyC, and MyCvol values compared with the normal right side (*B, red ROI*). The WM map (*C*) does not assign as the FASI; however, GM map (*D*) signs the FASI as GM.

which would have already been performed at the time of diagnosis. In addition, with the help of the obtained quantitative data on SyMRI, comparing the morphometric data annually during the shrinking or disappearing of the FASI may reduce the need for frequent follow-ups in these patients. However, in some situations requiring intermittent checkups, SyMRI could be very promising, giving additional quantitative information that can be useful in follow-up comparisons.

In our study, patients with NF-1 had a significantly higher ICV than HCs, similar to findings in several previous studies.[1,3,20] In the literature, BPV and WM volumes were higher and GM volumes were lower than our findings in patients with NF-1.[3] However, FASI were labeled and quantified as GM, which might have resulted in higher GM values in our patients with NF-1. Some studies[3,20] showed that the presence of an optic glioma might influence the mean brain volume in patients with NF-1, but patients with optic and/or brain gliomas were excluded from our study. Therefore, we believe that morphometric alterations in this study may reflect histopathologic abnormalities more accurately than in previous reports.

Morphometric MR imaging studies in NF-1 were limited to BPV, GM, and WM volumes.[3,20] Although the differences were not statistically significant, MY, MyF, and the non-GM/WM/CSF volumes tended to be higher in patients with NF-1 than in HCs. The MyV of the pons and R2 values of the caudate nucleus and thalami were significantly lower than those in HCs. Additionally, all values except PD were significantly decreased in FASI on myelin maps. These novel findings may point to underlying myelin and/or axonal structural changes, in line with the studies conducted in patients with multiple sclerosis.[21,22]

Diffusion tensor imaging has also been widely used to understand tissue changes in diseases.[23-26] Elevated ADC and reduced fractional anisotropy throughout the WM tracts in NF-1 suggest a compromise in the integrity of WM.[24,26,27] MR spectroscopy studies

suggest an underlying structural abnormality in NF-1, revealing metabolic alterations in both the NABP and FASI.[28,29] Furthermore, after the disappearance of FASI, fractional anisotropy was reduced in the thalamus, suggesting that a microstructural abnormality may remain.[30,31] Experimental and clinical imaging studies showed increased radial diffusivity with or without alterations in axial diffusivity in the NABP of patients with NF-1.[25,26] We did not observe significant abnormalities in the NABP group compared with HCs. However, the younger age of our patients compared with those in previous studies in the literature may explain this finding.

We found significantly decreased MyV, MyCvol, WM, WMFvol, R2, and R1 values in the FASI in myelin maps in the NF-1 group. These findings may also correspond with reported histologic abnormalities, including an increased amount of space in axonal packing (sparse packing), myelin decompaction, and increased myelin thickness[26] in patients with NF-1. Further investigations, including the correlation of histologic and molecular changes in myelin with SyMRI, are necessary.

Our study has several limitations. First, our patient population with NF-1 was small as a result of the inclusion criteria of our study. We included only pediatric patients to focus on changes in FASI, which are more prominent early in life. Patients with gliomas were excluded to eliminate the effect of the tumor on increased volume. A larger patient population may yield more significant results. Additionally, because SyMRI was performed on a limited number of pediatric patients, we could not evaluate possible volume changes across age groups, a finding that was shown previously.[3] However, considering the age range of the participants and our exclusion criteria, a noticeable sequential change in intracranial volume is not expected. In the GM map, assigning the FASI as part of the GM might have created a false increase in the total GM volume. Additionally, correlations between volume measures and neuropsychological performance, which were not available in this study, would enhance our understanding of morphologic alterations from a clinical perspective.

CONCLUSIONS

SyMRI provides quantitative information in patients with NF-1 in terms of altered morphometry and tissue metrics, providing insights into the disease effects on the brain. A major advantage of this technique is that it reveals multicontrast sequences in a single acquisition, offering a reasonable scan time for clinical use, especially in young children.

ACKNOWLEDGMENT

The authors would like to thank all the MR technicians, Synthetic MRI team, and Ali Avci from Siemens Healthineers, Turkey, for their contribution in performing this study.

Disclosures: Banu Anlar—UNRELATED: Consultancy: Novartis.

REFERENCES

1. Van Es S, North KN, McHugh K, et al. **MRI findings in children with neurofibromatosis type 1: a prospective study.** *Pediatr Radiol* 1996;26:478–87 CrossRef Medline
2. The I, Hannigan GE, Cowley GS, et al. **Rescue of a Drosophila NF1 mutant phenotype by protein kinase A.** *Science* 1997;276:791–94 CrossRef Medline
3. Moore BD 3rd, Slopis JM, Jackson EF, et al. **Brain volume in children with neurofibromatosis type 1: relation to neuropsychological status.** *Neurology* 2000;54:914–20 CrossRef Medline
4. López-Juárez A, Titus HE, Silbak SH, et al. **Oligodendrocyte Nf1 controls aberrant notch activation and regulates myelin structure and behavior.** *Cell Rep* 2017;19:545–57 CrossRef Medline
5. DiPaolo DP, Zimmerman RA, Rorke LB, et al. **Neurofibromatosis type 1: pathologic substrate of high-signal-intensity foci in the brain.** *Radiology* 1995;195:721–24 CrossRef
6. Menor F, Marti-Bonmati L, Arana E, et al. **Neurofibromatosis type 1 in children: MR imaging and follow-up studies of central nervous system findings.** *Eur J Radiol* 1998;26:121–31 CrossRef Medline
7. Warntjes JB, Leinhard OD, West J, et al. **Rapid magnetic resonance quantification on the brain: optimization for clinical usage.** *Magn Reson Med* 2008;60:320–29 CrossRef Medline
8. Krauss W, Gunnarsson M, Andersson T, et al. **Accuracy and reproducibility of a quantitative magnetic resonance imaging method for concurrent measurements of tissue relaxation times and proton density.** *Magn Reson Imaging* 2015;33:584–91 CrossRef Medline
9. Hagiwara A, Hori M, Yokoyama K, et al. **Utility of a multiparametric quantitative MRI model that assesses myelin and edema for evaluating plaques, periplaque white matter, and normal-appearing white matter in patients with multiple sclerosis: a feasibility study.** *AJNR Am J Neuroradiol* 2017;38:237–42 CrossRef Medline
10. Andica C, Hagiwara A, Nakazawa M, et al. **The advantage of synthetic MRI for the visualization of early white matter change in an infant with Sturge-Weber syndrome.** *Magn Reson Med Sci* 2016;15:347–48 CrossRef Medline
11. Virhammar J, Warntjes M, Laurell K, et al. **Quantitative MRI for rapid and user-independent monitoring of intracranial CSF volume in hydrocephalus.** *AJNR Am J Neuroradiol* 2016;37:797–801 CrossRef Medline
12. Krauss W, Gunnarsson M, Nilsson M, et al. **Conventional and synthetic MRI in multiple sclerosis: a comparative study.** *Eur Radiol* 2018;28:1692–700 CrossRef Medline
13. Sevick RJ, Barkovich AJ, Edwards MS, et al. **Evolution of white matter lesions in neurofibromatosis type 1: MR findings.** *AJR Am J Roentgenol* 1992;159:171–75 CrossRef Medline
14. Andica C, Hagiwara A, Hori M, et al. **Automated brain tissue and myelin volumetry based on quantitative MR imaging with various in-plane resolutions.** *J Neuroradiol* 2018;45:164–68 CrossRef Medline
15. Warntjes M, Engström M, Tisell A, et al. **Modeling the presence of myelin and edema in the brain based on multi-parametric quantitative MRI.** *Front Neurol* 2016;7:16 CrossRef Medline
16. Benjamini Y, Hochberg Y. **Controlling the false discovery rate: a practical and powerful approach to multiple testing.** *Journal of the Royal Statistical Society Series B* 1995;57:289–300
17. Blystad I, Warntjes JB, Smedby O, et al. **Synthetic MRI of the brain in a clinical setting.** *Acta Radiol* 2012;53:1158–63 CrossRef Medline
18. Tanenbaum LN, Tsiouris AJ, Johnson AN, et al. **Synthetic MRI for clinical neuroimaging: results of the Magnetic Resonance Image Compilation (MAGiC) prospective, multicenter, multireader trial.** *AJNR Am J Neuroradiol* 2017;38:1103–10 CrossRef Medline
19. Kerleroux B, Kober T, Hilbert T, et al. **Clinical equivalence assessment of T2 synthesized pediatric brain magnetic resonance imaging.** *J Neuroradiol* 2019;46:130–35 CrossRef Medline
20. Said SM, Yeh TL, Greenwood RS, et al. **MRI morphometric analysis and neuropsychological function in patients with neurofibromatosis.** *Neuroreport* 1996;7:1941–44 CrossRef Medline
21. West J, Aalto A, Tisell A, et al. **Normal appearing and diffusely abnormal white matter in patients with multiple sclerosis assessed with quantitative MR.** *PLoS One* 2014;9:e95161 CrossRef Medline
22. Saccenti L, Hagiwara A, Andica C, et al. **Myelin measurement using quantitative magnetic resonance imaging: a correlation study**

comparing various imaging techniques in patients with multiple sclerosis. *Cells* 2020;9:393 CrossRef Medline

23. Tognini G, Ferrozzi F, Garlaschi G, et al. **Brain apparent diffusion coefficient evaluation in pediatric patients with neurofibromatosis type 1.** *J Comput Assist Tomogr* 2005;29:298–304 CrossRef Medline
24. Zamboni SL, Loenneker T, Boltshauser E, et al. **Contribution of diffusion tensor MR imaging in detecting cerebral microstructural changes in adults with neurofibromatosis type 1.** *AJNR Am J Neuroradiol* 2007;1:773 Medline
25. Wang L, Goldstein FC, Veledar E, et al. **Alterations in cortical thickness and white matter integrity in mild cognitive impairment measured by whole-brain cortical thickness mapping and diffusion tensor imaging.** *AJNR Am J Neuroradiol* 2009;30:893–99 CrossRef Medline
26. Karlsgodt KH, Rosser T, Lutkenhoff ES, et al. **Alterations in white matter microstructure in neurofibromatosis-1.** *PLoS One* 2012;7:e47854 CrossRef Medline
27. Song SK, Sun SW, Ramsbottom MJ, et al. **Dysmyelination revealed through MRI as increased radial (but unchanged axial) diffusion of water.** *Neuroimage* 2002;17:1429–36 CrossRef Medline
28. Wilkinson ID, Griffiths PD, Wales JK. **Proton magnetic resonance spectroscopy of brain lesions in children with neurofibromatosis type 1.** *Magn Reson Imaging* 2001;19:1081–89 CrossRef Medline
29. Jones AP, Gunawardena WJ, Coutinho CM. **1H MR spectroscopy evidence for the varied nature of asymptomatic focal brain lesions in neurofibromatosis type 1.** *Neuroradiology* 2001;43:62–67 CrossRef Medline
30. Ferraz-Filho JR, da Rocha AJ, Muniz MP, et al. **Diffusion tensor MR imaging in neurofibromatosis type 1: expanding the knowledge of microstructural brain abnormalities.** *Pediatr Radiol* 2012;42:449–54 CrossRef Medline
31. van Engelen SJ, Krab LC, Moll HA, et al. **Quantitative differentiation between healthy and disordered brain matter in patients with neurofibromatosis type I using diffusion tensor imaging.** *AJNR Am J Neuroradiol* 2008;29:816–22 CrossRef Medline